All n-3 PUFA are not the same: MD simulations reveal differences in membrane organization for EPA, DHA and DPA

Xiaoling Leng[a,b], Jacob J. Kinnun[a], Andres T. Cavazos[a], Samuel W. Canner[a,c], Saame Raza Shaikh[d], Scott E. Feller[e] and Stephen R. Wassall[a]

[a]Department of Physics, IUPUI, Indianapolis, IN 46202-3273

[c]Department of Computer Science and Information Science,
IUPUI, Indianapolis, IN 46202-5132

[d]Department of Nutrition, Gillings School of Global Public Health and School of Medicine,
The University of North Carolina at Chapel Hill, Chapel Hill, NC 27599

and

[e]Department of Chemistry, Wabash College, Crawfordsville, IN 47933

Email for correspondence swassall@iupui.edu

[b]Present address Institute of Molecular Biophysics, Florida State University, Tallahassee, FL 32306-4380

This is the author's manuscript of the article published in final edited form as:
Leng, X., Kinnun, J. J., Cavazos, A. T., Canner, S. W., Shaikh, S. R., Feller, S. E., & Wassall, S. R. (2017). All n-3 PUFA are not the same: MD simulations reveal differences in membrane organization for EPA, DHA and DPA. Biochimica et Biophysica Acta (BBA) - Biomembranes. https://doi.org/10.1016/j.bbamem.2018.01.002

ABSTRACT

Eicosapentaenoic (EPA, 20:5), docosahexaenoic (DHA, 22:6) and docosapentaenoic (DPA, 22:5) acids are omega-3 polyunsaturated fatty acids (n-3 PUFA) obtained from dietary consumption of fish oils that potentially alleviate the symptoms of a range of chronic diseases. We focus here on the plasma membrane as a site of action and investigate how they affect molecular organization when taken up into a phospholipid. All atom MD simulations were performed to compare 1-stearoyl-2-eicosapentaenoylphosphatylcholine (EPA-PC, 18:0-20:5PC), 1-stearoyl-2-docosahexaenoylphosphatylcholine (DHA-PC, 18:0-22:6PC), 1-stearoyl-2-docosapentaenoylphosphatylcholine (DPA-PC, 18:0-22:5PC) and, as a monounsaturated control, 1-stearoyl-2-oleoylphosphatidylcholine (OA-PC, 18:0-18:1PC) bilayers. They were run in the absence and presence of 20 mol% cholesterol. Multiple double bonds confer high disorder on all three n-3 PUFA. The different number of double bonds and chain length for each n-3 PUFA moderates the reduction in membrane order exerted (compared to OA-PC, $\bar{S}_{CD}$ = 0.152). EPA-PC ($\bar{S}_{CD}$ = 0.131) is most disordered, while DPA-PC ($\bar{S}_{CD}$ = 0.140) is least disordered. DHA-PC ($\bar{S}_{CD}$ = 0.139) is, within uncertainty, the same as DPA-PC. Following the addition of cholesterol, order in EPA-PC ($\bar{S}_{CD}$ = 0.169), DHA-PC ($\bar{S}_{CD}$ = 0.178) and DPA-PC ($\bar{S}_{CD}$ = 0.182) is increased less than in OA-PC ($\bar{S}_{CD}$ = 0.214). The high disorder of n-3 PUFA is responsible, preventing the n-3 PUFA-containing phospholipids from packing as close to the rigid sterol as the monounsaturated control. Our findings establish that EPA, DHA and DPA are not equivalent in their interactions within membranes, which possibly contributes to differences in clinical efficacy.

Keywords: phospholipid chain order, cholesterol, unsaturated fatty acids, fish oils

Abbreviations

[1]docosahexaenoic acid (DHA), docosapentaenoic (DPA), eicosapentaenoic acid (EPA), electron density profile (EDP), number density profile (NDP), oleic acid (OA), omega-3 polyunsaturated fatty acid(s) (n-3 PUFA), phosphatidylcholine (PC), radial distribution function (RDF), stearic acid (SA), 1,2-dioleolylphosphatidylcholine (DOPC), 1-palmitoyl-2-oleoylphosphatidylcholine (POPC), 1-stearoyl-2-docosahexaenoylphosphatidylcholine (DHA-PC), 1-stearoyl-2-docosapentaenoylphosphatidylcholine (DPA-PC), 1-stearoyl-2-eicosapentaenoylphosphatidylcholine (EPA-PC), 1-stearoyl-2-oleoylphosphatidylcholine (OA-PC)

1. INTRODUCTION

Long chain omega-3 polyunsaturated fatty acids (n-3 PUFA)[1] are a distinct class of fatty acids that have multiple double bonds, with the last double bond being located 3 carbons from the terminal methyl (n or ω) end of the chain [1]. They began to attract attention in the 1970's when a low incidence of cardiovascular disease was noted in the Inuit population who consumed a diet rich in oily fish that contain an abundance of n-3 PUFA [2]. Since then many more health benefits have been discovered including the treatment of neurological problems [3], relief of the symptoms of inflammatory disorders [4], improvements in whole body metabolism [5] and prevention of the progress of certain cancers [6]. The major source of long chain n-3 PUFA in the diet is oily cold-water fish and/or extracted oil supplements [1]. Eicosapentaenoic acid (EPA, 20:5) with 20 carbons and 5 double bonds at the 5, 8, 11, 14 and 17 positions and docosahexaenoic acid (DHA, 22:6) with 22 carbons and 6 double bonds at the 4, 7, 10, 13, 16 and 19 positions are the primary ones. Present in smaller concentration, and to which EPA often converts, is docosapentaenoic acid (DPA, 22:5) with 22 carbons and 5 double bonds at the 7, 10, 13, 16 and 19 positions. DPA has only recently begun to be the subject of research, in contrast to EPA and DHA that have been widely studied [7]. Although all three n-3 PUFA are similar in chemical structure, whether they have similar, unique or complementary impact upon health remains a matter of debate [8].

A complete explanation of the mode of action for n-3 PUFA currently does not exist. Modulation of the organization of plasma membranes following the uptake of n-3 PUFA into

phospholipids is among the potential mechanisms that have been identified [9-11]. The basic idea is a variation on the lipid raft concept [12]. According to this model, predominantly saturated sphingolipids and cholesterol segregate into tightly packed nanodomains that coalesce into functional microdomains (rafts) within a surrounding phospholipid environment that is less ordered. By incorporating into membrane phospholipids, highly disordered n-3 PUFA that have an aversion for cholesterol are then proposed to manipulate the composition and structure of the domains. One example of a scenario envisaged, for instance, has the introduction of n-3 PUFA-containing phospholipids into a raft displacing cholesterol and breaking apart the domain [11]. Detergent extraction assays and imaging studies performed on cells either treated with n-3 PUFA or obtained following a n-3 PUFA enriched diet support the general premise that n-3 PUFA are taken up into rafts and affect their size [13,14]. Changes in the levels of other fatty acids due to cellular metabolism, however, complicate interpretation. A series of studies on biomimetic membranes of controlled composition carried out in our laboratories have started to provide insight [15-18]. They established that the partitioning of an n-3 PUFA-containing phospholipid between more ordered raft-like and less ordered non-raft environments is sensitive to molecular structure. A much greater tendency for DHA- than EPA-containing phosphatidylcholine (PC) to infiltrate raft-like domains was revealed, which we attribute to a differential in the disorder associated with DHA relative to EPA and speculate may indicate a variance in bioactivity. To better understand this behavior and the possible role that the structure of an individual n-3 PUFA plays in determining biological activity, we have run atomistic MD simulations to make a direct comparison of EPA, DHA and DPA and their interaction with

cholesterol.

All atom MD simulation opens up a perspective on molecular structure and dynamics within lipid membranes that is unprecedented in detail [19]. The reliability of this computational method has been ascertained in tests on well-characterized systems that successfully reproduce experimental measurements. It is an approach that has been tremendously influential in developing a comprehension of the physical properties of PUFA-containing phospholipids. Simulations published for DHA-containing PC bilayers more than a decade ago were instrumental in showing that the polyunsaturated chain is highly flexible, rapidly undergoing isomerization between conformations that include extended and bent configurations [20-22]. A reduced energy barrier for rotation about the single bonds in the recurring =C-C-C= unit possessed by PUFA is responsible, debunking an alternative view that the rigidity of multiple bonds would produce low flexibility. Subsequent analysis of simulations on a 1-stearoyl-2-docosahexaenoylphosphatidylcholine (18:0-22:6PC, DHA-PC) bilayer in the presence of cholesterol showed that the steroid moiety prefers close proximity to the saturated stearic acid (SA) chain over the polyunsaturated DHA chain [23]. This finding corroborates an arrangement inferred from experimental measurements of the orientation of cholesterol and its solubility in polyunsaturated membranes [24]. Phenomenal disorder that pushes cholesterol away is what distinguishes PUFA and renders membrane architecture particularly responsive to their presence.

An investigation of how molecular organization in lipid bilayers is affected by differences in the structure of EPA, DHA and DPA is presented here. To this end, we performed atomistic

MD simulations comparing 1-stearoyl-2-eicosapentaenoylphosphatidylcholine (18:0-20:5PC, EPA-PC), 1-stearoyl-2-docosahexaenoylphosphatidylcholine (18:0-22:6PC, DHA-PC, 1-stearoyl-2-docosapentaenoylphosphatidylcholine (18:0-22:5PC, DPA-PC) and 1-stearoyl-2-oleoylphosphatidylcholine (18:0-18:1PC, OA-PC) bilayers. Their molecular

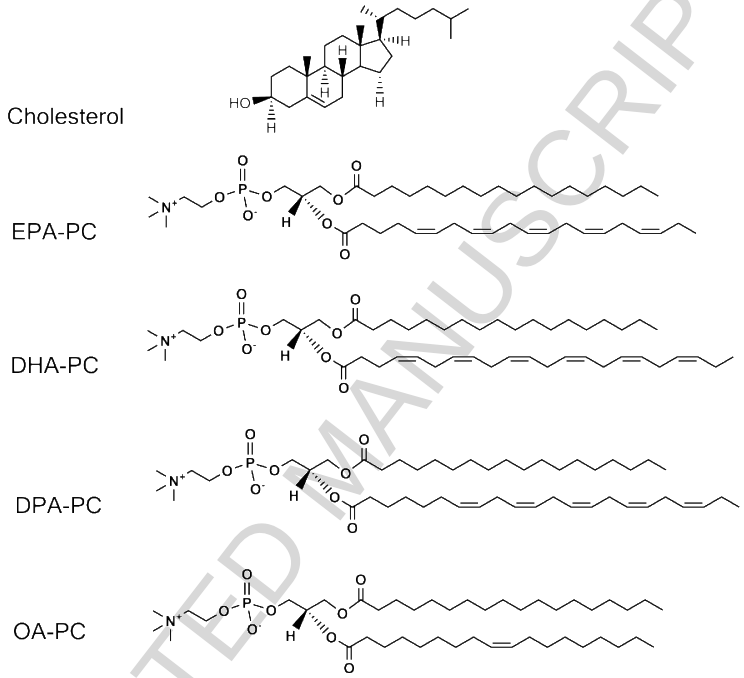

structure, together with cholesterol, is shown in Figure 1. DHA-PC, EPA-PC and DPA-PC are

Figure 1 Molecular structure of OA-PC, DPA-PC, DHA-PC, EPA-PC and cholesterol.

representative of a phospholipid into which n-3 PUFA have been taken up in the plasma membrane, while OA-PC serves as a monounsaturated control [25]. In a structural motif that is typical of phospholipids found in animal membranes, they all have SA, a common saturated fatty acid, at the *sn*-1 position and an unsaturated fatty acid at the *sn*-2 position. The simulations were

run on single component membranes and in the presence of 20 mol% cholesterol to characterize interaction with the sterol for each n-3 PUFA. Supplementary solid state ^{2}H NMR experiments employing analogs of the phospholipids perdeuterated in the *sn*-1 chain were conducted for validation.

2. MATERIALS AND METHODS

2.1 MD simulations

Atomistic MD simulations were performed on DHA-PC, EPA-PC, DPA-PC and OA-PC bilayers in the absence and presence of 20 mol% cholesterol. They were run in the constant particle number, pressure and temperature (NPT) ensemble. There were 98 PC molecules in the single component membrane simulations, and 80 PC molecules and 20 cholesterol molecules in the two-component membrane simulations. In each case, the membrane was hydrated with 2000 water molecules. The initial structure of OA-PC, OA-PC + cholesterol, DHA-PC and DHA-PC + cholesterol bilayers was assembled with the CHARMM-GUI Membrane Builder [26]. Then, by modifying the DHA chain on DHA-PC molecules, the initial structure of EPA-PC + cholesterol and DPA-PC + cholesterol bilayers was generated from our assembled DHA-PC + cholesterol bilayer. Locating the corresponding lipid molecule into a bilayer grid with a customized script created the initial structure of EPA-PC and DPA-PC bilayers. This approach avoided atom/chain conflicts that appear in the initial structure when it is directly modified from the assembled DHA-PC bilayer. All simulations were run using the CHARMM C36p force field [27]. Non-bonded (van der Waals and short-range electrostatic) interactions were gradually switched

off at 10 Å, and the long-range electrostatic interactions were calculated using the particle-mesh Ewald method [28]. The membranes were equilibrated with the standard CHARMM-GUI six-step process over 200 ps [26] during which constraints on lipids were gradually released [29].

Production runs of our simulations were performed with NAMD [30] on the Big Red II super computer at Indiana University. Each one was run over 200 ns using a time step of 2 fs, with the first 20 ns considered to be equilibration. In all simulations, periodic boundary conditions were applied to a rectangular box on which the x and y dimensions (in the plane of the membrane) were kept equal while the z dimension (in the direction of the membrane normal) was varied independently. The temperature was kept at 37 °C and the pressure was maintained at 1 atm by the Langevin dynamics piston method [31]. Analyses of simulations, including calculating order parameters and densities of atoms in 1- and 3-dimensions were achieved with customized Tcl script executed in the visual molecular dynamics (VMD) program [32]. Snapshots of bilayers and illustrations were also created with VMD, and rendered by blender.

2.2 Solid state ^{2}H NMR

Details of solid state ^{2}H NMR experiments are provided in Supporting Information.

3. RESULTS AND DISCUSSION

Biological membranes contain a diverse array of lipids. Phospholipids vary in head group and chain composition – number of carbons and number and location of double bonds. These variations in molecular structure modify physical properties and molecular organization within a

membrane in a complex manner. The aim of our study is to focus on three n-3 PUFA - EPA, DHA and DPA. With MD simulations performed on EPA-PC, DHA-PC and DPA-PC, we observe how they affect the molecular organization of a phospholipid bilayer. OA-PC, a common monounsaturated phospholipid, is employed as a benchmark for comparison.

3.1 Molecular organization in single component membranes

From our simulations on EPA-PC, DHA-PC and DPA-PC bilayers, differences in how each n-3 PUFA affects acyl chain order within membranes and the thickness of a bilayer were identified.

3.1.1 Membrane order

The order parameter S_{CD} is a fundamental quantity describing the dynamics of acyl chain segments in a membrane that is accessible by MD simulations and solid state ^{2}H NMR spectroscopy [33]. It is a measure of the anisotropy of motion for the C-H (H is replaced by ^{2}H in ^{2}H NMR experiments) bond on a methylene or methyl group in an acyl chain. The definition of the order parameter is

$$S_{CD} = \tfrac{1}{2}\langle 3\,cos^2\,\beta - 1\rangle \qquad (1)$$

where β is the angle between the C-H bond on a particular chain segment and the membrane normal about which the reorientation of the chain is axially symmetric [34]. The angular brackets signify a time average that is also taken over all the molecules in a simulation. In the case of methylene groups and the terminal methyl group, an average order parameter for the two and three C-H bonds in the respective segments is usually calculated. An exception is the two C-H

bonds on the methylene group at the C2 position of the *sn*-2 chain for which constraints on orientation due to the glycerol backbone lead to order parameters that are unequal [35]. A range $0 \leq |S_{CD}| \leq 0.5$ typically applies to the value for S_{CD} [18]. The upper limit corresponds to a methylene group undergoing fast axial rotation in an all-trans chain (β = 90°) while the lower limit corresponds to isotropic motion (β takes all angles) for a methylene or methyl group.

Figure 2 (upper panel) shows the order parameter profiles obtained from simulation along the saturated SA chain at the *sn*-1 position in EPA-PC, DHA-PC, DPA-PC and OA-PC. They all display a form that is a signature for saturated phospholipid acyl chains in the lamellar liquid

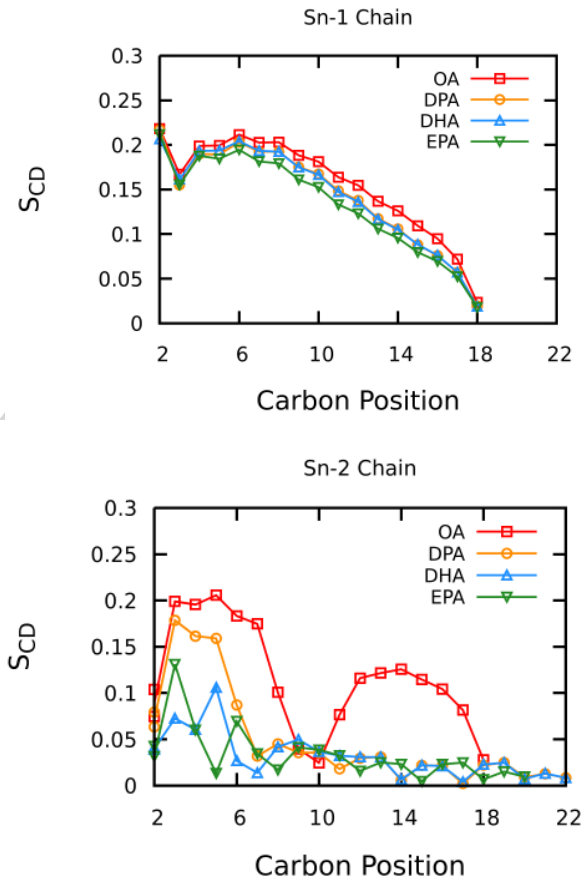

Figure 2 Order parameter profile along the *sn*-1 (upper panel) and -2 (lower panel) chains in OA-PC (red), DPA-PC (yellow), DHA-PC (blue) and EPA-PC (green) bilayers obtained from

MD simulations at 37°C. The uncertainty in the S_{CD} values is ≤±0.003, which was estimated from the standard error obtained treating each lipid molecule independently.

crystalline phase [34]. In the top half of the chain the S_{CD} values exhibit a plateau region of approximately constant order (S_{CD} ~ 0.2, C4-C8 positions), and then progressively decrease in the bottom half toward the terminal methyl group (S_{CD} ~ 0.02, C18 position) near the center of bilayer. Reorientation is constrained by tighter packing in the upper portion where the chain is anchored at the hydrophilic interface, while in the lower portion there is increasingly less restriction to motion towards the free end at the foot of the chain. Inspection of the profiles reveals the reduction in order expected to accompany the presence of a polyunsaturated *sn*-2 chain, which we quantify in terms of an average order parameter $\bar{S}_{CD}$ that represents the global effect on the entire *sn*-1 chain (Table 1). Among the PUFA-containing phospholipids, EPA-PC ($\bar{S}_{CD}$ = 0.131) is the most disordered while DPA-PC ($\bar{S}_{CD}$ = 0.140) is the least disordered. DHA-PC ($\bar{S}_{CD}$ = 0.139) is, within uncertainty, the same as DPA-PC. They are all ~10% less ordered than monounsaturated OA-PC ($\bar{S}_{CD}$ = 0.152).

Table 1 Average order parameters $\bar{S}_{CD}$ for the *sn*-1 and -2 chains in OA-PC, DPA-PC, DHA-PC and EPA-PC membranes without and with 20 mol% of cholesterol. The uncertainty in the $\bar{S}_{CD}$ values is <±0.002, which was estimated from the standard error obtained treating each lipid molecule independently.

Phospholipid	$\bar{S}_{CD}$			
	sn-1		*sn*-2	
	Without Cholesterol	With cholesterol	Without Cholesterol	With cholesterol
OA-PC	0.152	0.214	0.119	0.170
DPA-PC	0.140	0.182	0.047	0.062
DHA-PC	0.139	0.178	0.030	0.041

EPA-PC	0.131	0.169	0.032	0.044

The trends seen here are consistent with those observed experimentally by ^{2}H NMR with analogs of PC deuterated in the *sn*-1 chain. Order parameter profiles published for the SA *sn*-1 chain in a series of PC membranes as a function of the level of unsaturation in the *sn*-2 chain demonstrated that increasing the number of double bonds from 1 to 3 substantially decreases order [36]. Thereafter the changes in order on increasing the number of double bonds from 3 to 6 are modest. The hierarchy of disorder EPA-PC (most disordered) > DHA-PC ≥ DPA-PC (least disordered) identified by simulation qualitatively reproduces the variation of the average order parameter previously measured by us using moment analysis [37] and of the smoothed order parameter profiles constructed from FFT depaked spectra in the current work (Figures S1, S2 and Table S1 in Supporting Information). An order parameter profile has not been reported, as far as we know, for DPA-PC before. To give context to the potential significance of the modest difference in order parameter observed here between n-3 PUFA-containing phospholipids, order parameters that differ by a comparable amount were reported in earlier work contrasting the properties for bilayers composed of n-3 vs. n-6 (where the last double is 6 carbons from the terminal methyl group) PUFA-containing phospholipids. [38,39].

The order parameters that were calculated for the unsaturated *sn*-2 chain in EPA-PC, DHA-PC, DPA-PC and OA-PC are plotted as function of position in Figure 2 (lower panel). Not surprisingly, there is a big difference between the OA chain and PUFA chains. The OA chain in OA-PC has a profile that is similar to the SA *sn*-1 chain, apart from positions C8-C11 where

there is big drop in the magnitude of S_{CD}. This phenomenon was first observed experimentally and is understood [40,41]. A localized region of enhanced segmental motion within the OA chain is not the reason for the reduced order parameters. The configuration of the chain around the rigid *cis* double bond, instead, produces a most probable orientation for which the order parameters of the C-H bonds on the chain segments at (C9 and C10) and flanking (C8 and C11) the double bond are inherently low – i.e. β takes angles near the "magic" angle (54.7°) at which the second order Legendre polynomial in the definition of the order parameter (eq. 1) goes to zero.

Compared to the OA chain in OA-PC, the order parameters for the PUFA chain in EPA-PC, DHA-PC and DPA-PC are much lower. They are less than 0.05 throughout the bottom two-thirds of the chain (C7 to the end), which is comparable to the value of S_{CD} for the highly mobile methyl group at the free end of a chain. An almost uniform distribution from 0 to 180° for the value of the angle β that the C-H bonds make with the bilayer normal is responsible. The truly high disorder implied is the result of the shallow energy barrier to rotation about C-C bonds in the repeating =CH-CH_2-CH= motif that distinguish PUFA with their multiple double bonds from less unsaturated fatty acids [42]. This behavior is well documented by simulation and experiment in the case of DHA [26,43-45]. Higher order exists in the uppermost portion of the PUFA chains before the sequence of double bonds begins. The effect is most pronounced in DPA where the first double bond does not occur until carbon C7 (Figure 1). The order parameter (S_{CD} ~ 0.17) at positions C3-5 of the DPA chain in DPA-PC approaches the value seen at the same positions for OA in OA-PC (S_{CD} ~ 0.20) (Figure 3). A similar plateau-like region of

elevated order is found in the profile for neither DHA in DHA-PC nor EPA in EPA-PC. We attribute its presence in DPA to the removal of the double bond at the C4 position relative to DHA and to the addition of two methylene groups prior to the first double bond relative to EPA (Figure 1). In response, order parameters in the SA *sn*-1 chain are higher for DPA-PC than DHA-PC and, to greater extent, EPA-PC. The lower order of the SA chain in EPA-PC than DHA-PC indicates that, as we have previously surmised [37], the ordering associated with the loss of a double bond is more than compensated by the disordering associated with the shortening of the chain on replacing DHA by EPA. Whether this observation is specific to EPA vs. DHA or more generally applicable remains to be seen.

3.1.2 Membrane thickness

Electron density profiles (EDP) that were calculated across the membrane for EPA-PC, DHA-PC, DPA-PC and OA-PC are shown in Figure 3 (upper panel). They were generated from histograms of the atoms in lipids along the bilayer normal (z direction) that were weighted by the number of electrons associated with each atom. Because the area of membrane that was simulated is too small to undulate, the z direction in our system well represents the membrane normal [46]. In the EDP of each membrane, there is a dip in the middle (z = 0) of the bilayer reflecting where the highly disordered methyl groups at the end of acyl chains reside. The peaks on both sides correspond to the electron dense head group at the edge of the membrane and, as illustrated (Fig. 3, upper panel), approximate to the location of the phosphate group. Their separation is commonly taken to be the membrane thickness [47] and was used by us to determine the D_{HH} values listed in Table 2. The agreement with experimental data that exist in

the literature for OA-PC (38.7 Å) [48] and DHA-PC (37.9 Å) [38] is good (within 1 Å). As far we know D_{HH} has not been measured for EPA-PC and DPA-PC, although in the latter case a thickness has been reported from X-ray work for its n-6 isomeric counterpart DPA(n-6)-PC (37.9 Å) [38].

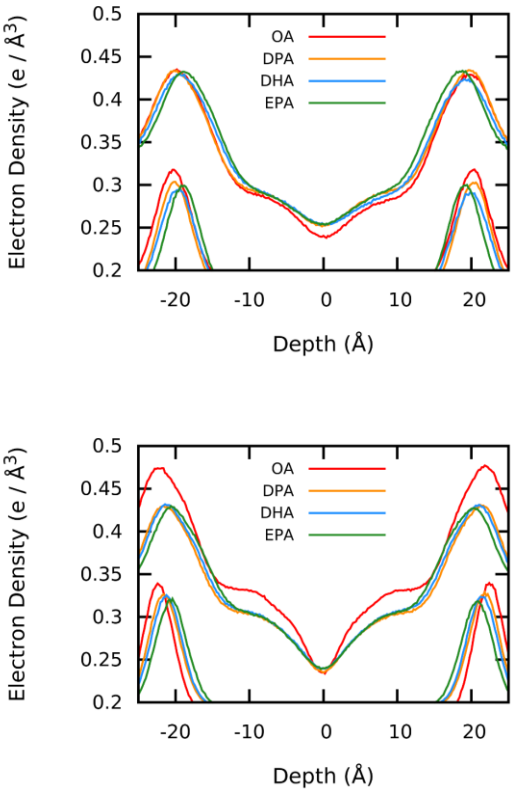

Figure 3 EDP for all atoms (above) and the number density profile of the phosphorus atom (below) on the phospholipid in OA-PC, DPA-PC, DHA-PC and EPA-PC bilayers without cholesterol (upper panel) and with addition of 20 mol% cholesterol (lower panel). The phosphate curves are vertically scaled and shifted for clarity. Table 2 gives the differences in membrane thickness D_{HH} calculated from the separation of the phosphate peaks.

It is generally recognized that introducing double bonds into a phospholipid chain causes a thinning of the bilayer [49]. A lipid chain with a double bond, and more markedly with multiple double bonds, is more disordered and occupies a larger cross-sectional area than a

saturated chain with same number of carbons. The result is a thinner bilayer. The measurements of membrane thickness obtained from our simulations conform to the gist of this view (Table 2). They demonstrate that DPA-PC, DHA-PC (22 carbons) and EPA-PC (20 carbons) with a polyunsaturated *sn*-2 chain are comparable in thickness or thinner than OA-PC (18 carbons) with a shorter monounsaturated *sn*-2 chain. As an aside, we point out that the values of D_{HH} measured from the EDP generated from our simulations underscore that care should be exercised when relating the average order parameter for the saturated *sn*-1 chain (Table 1) to membrane thickness. The basic idea connecting the two parameters is that a more ordered *sn*-1 chain has a bigger projected length, corresponding to greater bilayer thickness [50]. However, despite an average order parameter for the SA *sn*-1 chain in DPA-PC that is almost 10% lower than in OA-PC, the thickness of the n-3 PUFA containing bilayer is slightly bigger. The length of the *sn*-2 chain is clearly a factor.

	OA-PC	DPA-PC	DHA-PC	EPA-PC
Pure	39.6	39.7	38.8	37.5
With cholesterol	44.2	42.9	42.2	40.7
Change	4.6	3.2	3.4	3.2

Table 2 Membrane thickness (D_{HH}) measured from phosphate-phosphate distance (Å) for OA-PC, DPA-PC, DHA-PC and EPA-PC in the absence and presence of 20 mol% cholesterol. The uncertainty is ±0.09 Å, estimated from the standard error of the peak locations.

3.2 Molecular organization in membranes containing cholesterol

From simulations run in the presence of 20 mol% cholesterol, we compared how acyl

chain order within the membrane and the thickness of the bilayer were affected in EPA-PC, DHA-PC and DPA-PC. To further assess interaction with the sterol, the location and orientation of cholesterol within the bilayers were determined and the distribution of each chain around the steroid moiety was mapped.

3.2.1 Membrane order

The addition of 20 mol% cholesterol to EPA-PC, DHA-PC and DPA-PC produces the anticipated increase in order within the bilayer [51]. Order parameters are elevated along the entire SA chain at *sn*-1 position in each case, reflecting the constraint upon reorientation imposed by the rigid sterol molecule (Figure 4, upper panel). The shape of the profile remains largely unchanged. There is still a relatively flat region of approximately constant order parameter in the upper portion of the chain before order drops off in the lower portion towards the terminal methyl group. As judged by estimates of the average order parameter (Table 1), all three n-3 PUFA containing bilayers undergo essentially the same rise in order ($\Delta\bar{S}_{CD} \approx 0.040$) due to cholesterol so that the hierarchy of order between them is retained - DPA-PC ($\bar{S}_{CD}$ = 0.182) > DHA-PC ($\bar{S}_{CD}$ = 0.178) > EPA-PC ($\bar{S}_{CD}$ = 0.169). The sterol-induced ordering is less than seen for the SA chain in OA-PC ($\bar{S}_{CD}$ = 0.214 and correspondingly $\Delta\bar{S}_{CD}$ = 0.062). A greater differential in order between the n-3 PUFA- and OA-containing bilayers results, which is apparent on inspection of the profiles obtained with (Fig. 4, upper panel) and without (Fig. 2, upper panel) cholesterol. It has similarly been surmised from experimental results presented in earlier studies there is a smaller increase in order due to cholesterol for polyunsaturated vs. monounsaturated bilayers [52,53].

The response to the introduction cholesterol observed by simulation, moreover, captures the essence of the changes in order for the SA *sn*-1 chain exhibited in the ^{2}H NMR experiments on the various membranes that we performed to provide validation (Figures S3, S4 and Table S1

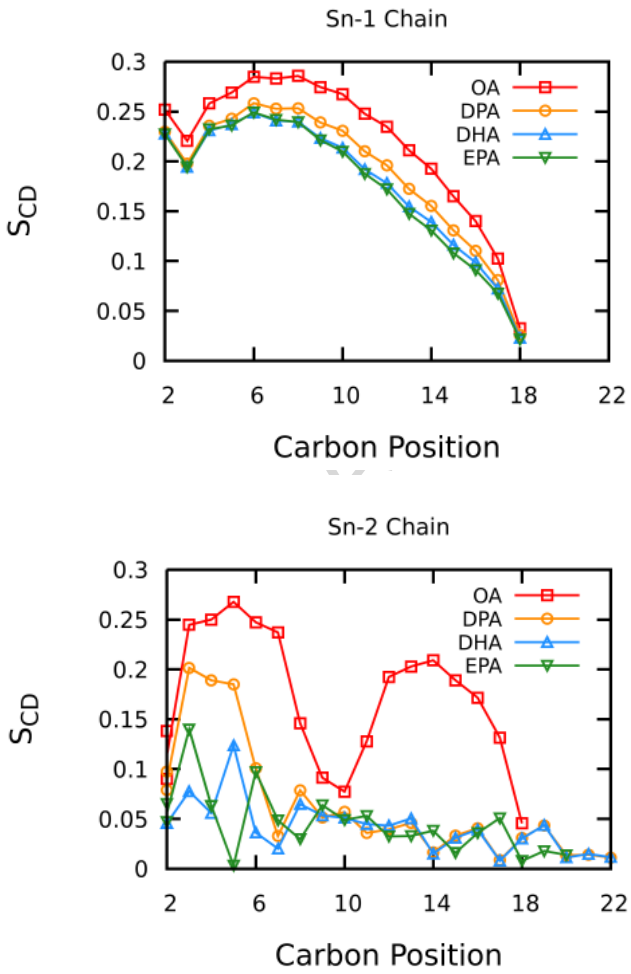

Figure 4 Order parameter profile along the *sn*-1 (upper panel) and -2 (lower panel) chains in OA-PC (red), DPA-PC (yellow), DHA-PC (blue) and EPA-PC (green) bilayers following the addition of 20 mol% cholesterol obtained from MD simulations at 37°C. The uncertainty in the S_{CD} values is ≤±0.003, which was estimated from the standard error obtained treating each lipid molecule independently. A comparative plot directly showing the effects of cholesterol on each profile is presented in Figure S6 (Supporting Information).

in Supporting Information). As with the simulated profiles, the experimentally derived profiles

for all three n-3 PUFA register a similar increase in order due the sterol that is smaller than for OA-PC.

A substantially more modest increase in order occurs for the n-3 PUFA chain at the *sn*-2 position in EPA-PC, DHA-PC and DPA-PC following the introduction of cholesterol than for the SA chain at the *sn*-1 position (Fig. 4, lower panel). The shift in average value for the order parameter ($\Delta\bar{S}_{CD}$ < 0.015) is correspondingly smaller and comparable in each case (Table 1). There is little change in the overall shape of the profile. Despite the presence of the rigid steroid moiety, the n-3 PUFA chains are still highly disordered with order parameters that are low throughout much of their length (S_{CD} < 0.08 in the bottom two thirds). High conformational flexibility, which allows PUFA chains to rapidly move through a diverse collection of configurations that include ones that have chain segments turning upside down, is responsible [23]. The chain segments in a PUFA chain at the *sn*-2 position are able to redistribute from the aqueous interfacial towards the hydrophobic interior in the presence of cholesterol with much less increase in order parameter than a saturated chain at the *sn*-1 position that is more restricted in conformation. In contrast, the order of the OA *sn*-2 chain in OA-PC is elevated to a much greater extent by cholesterol. It increases by an amount ($\Delta\bar{S}_{CD}$ = 0.051) approaching that undergone by the saturated SA *sn*-1 chain, retaining the form of the profile observed in the absence of the sterol. The effect of cholesterol on the order parameter profile for the DHA *sn*-2 chain in DHA-PC derived from our simulations parallels the results obtained from NMR spectra [53]. Experimental measurements of the order parameter in the OA *sn*-2 chain of OA-PC are too sparse to make a meaningful comparison, while we are unaware that order parameters in either

the EPA *sn*-2 chain of EPA-PC or DPA *sn*-2 chain of DPA-PC have been experimentally determined.

3.2.2 Membrane thickness

A thickening of EPA-PC, DHA-PC and DPA-PC, as well as of OA-PC, that follows the introduction of cholesterol is evident in the EDP constructed in Figure 3 (lower panel). It is a manifestation of the condensing effect of the sterol - the projected length of phospholipid chains ordered by cholesterol is greater and the bilayer becomes thicker [54]. All three of the n-3 PUFA-containing membranes undergo a comparable increase in thickness (ΔD_{HH} = 3.2-3.4 Å) that is less than the change undergone by the OA-containing membrane (ΔD_{HH} = 4.6 Å) (Table 2). As would be expected, the magnitude of these changes qualitatively parallels the elevation in molecular ordering due to cholesterol (Table 1). In agreement with these simulation-based findings, that the sterol produces a smaller increase in the width of DHA-PC compared to OA-PC bilayers may be gleaned from reports of neutron and x-ray scattering data [53,54].

3.2.3 Location of cholesterol

Cholesterol usually resides in a membrane with the hydroxyl group at one end of the tetracyclic ring near the aqueous interface while the short chain at the opposite end extends towards the center of the membrane [51]. An exception is bilayers that are thin (D_{HH} < 30 Å) in which hydrophobic mismatch drives the sterol into the interior of membrane where it straddles both leaflets [49]. This latter situation does not apply to the systems in the current study. The partial EDP generated from the simulated data for [2,3,4]- and [25,26,27]-carbons on cholesterol in EPA-PC, DHA-PC, DPA-PC and OA-PC conform to the canonical arrangement (Fig. 5, upper

and middle panels). They place the head ([2,3,4]-carbons) and tail ([25,26,27]-carbons) of the sterol, respectively, just below the surface and in the middle of the bilayer.

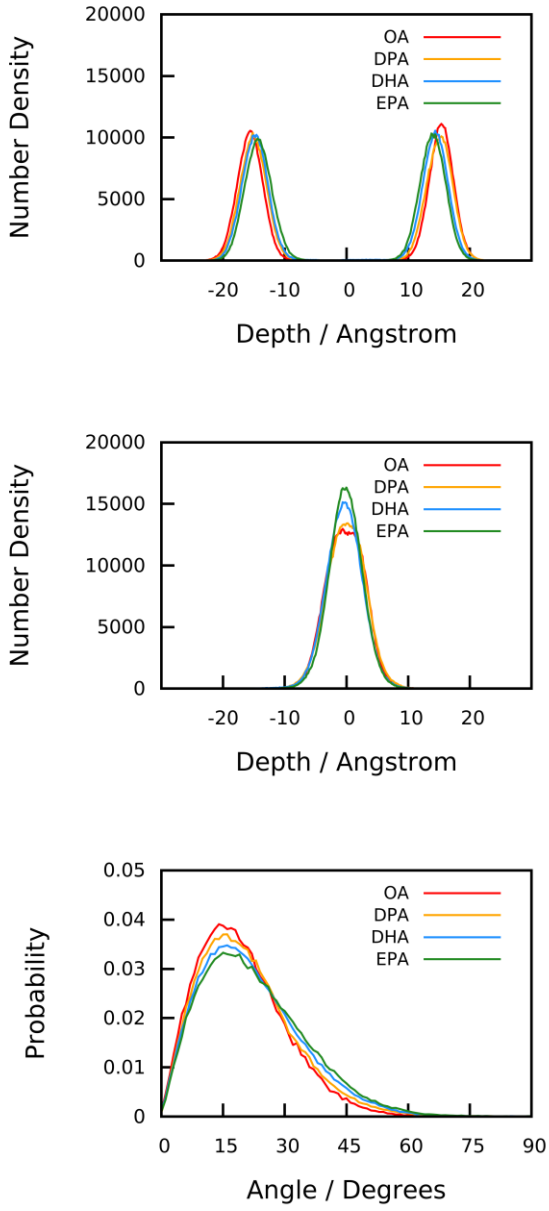

Figure 5 Carbon number density profile for the [2,3,4]-carbons (head group) and

[25,26,27]-carbons (tail) on cholesterol (upper and middle panels, respectively) and histogram of the orientation of cholesterol (vector connecting the C13-C10 carbons) relative to the bilayer normal (lower panel) in OA-PC, DPA-PC, DHA-PC and EPA-PC bilayers.

3.2.4 Orientation of cholesterol

The motion of cholesterol can be modeled as a fast rotation about the bilayer normal for the long molecular axis that in addition fluctuates in direction about a most probable orientation (tilt angle) offset from the normal [55]. Figure 5 (lower panel) shows the probability distribution calculated here for the angle a vector connecting the C13-C10 carbons, designating the alignment of the steroid moiety, makes with the bilayer normal in EPA-PC, DHA-PC, DPA-PC and OA-PC. A shift to larger angle and a broadening of the entire distribution accompanies the increase in disorder on replacing OA by each n-3 PUFA. It is clear, however, that there is little variation (< 2°) in the most probable orientation, denoted by the maximum in the distribution, between the various systems (Table 3). This observation is consistent with ^{2}H NMR work on

	OA-PC	DPA-PC	DHA-PC	EPA-PC
Most probable orientation	14.5°	15.2°	15.8°	16.4°
S_{CD}	0.37	0.36	0.35	0.35

Table 3 Most probable orientation for a vector connecting the C13-C10 carbons and the order parameter for the 3α C-H bond of cholesterol incorporated at 20 mol% into OA-PC, DPA-PC, DHA-PC and EPA-PC. The standard errors in tilt angle are ±0.2° (OA-PC), ±0.8° (DPA-PC), ±0.3° (DHA-PC) and ±0.4° (EPA-PC); and in order parameter are <±0.005.

[3α-^{2}H$_1$]cholesterol, an analog of the sterol labeled at the 3α position, incorporated at 50 mol% into PC bilayers with SA at the *sn*-1 position [56]. A tilt angle that is almost independent of the

level of unsaturation for the sn-2 chain was revealed by an analysis of order parameters measured for the 3α C-^{2}H bond in these experiments. The order parameters calculated from our simulations (Table 3), moreover, replicate the values measured by experiment for OA-PC (S_{CD} = 0.36) and DHA-PC (S_{CD} = 0.35). As far as we know, experimental data on [3α-$^2H_1$]cholesterol in DPA-PC and EPA-PC do not exist.

3.2.5 Interaction of cholesterol with acyl chains

As a molecule that orders the membrane, cholesterol does so by interacting with the nearby fatty acid chains. The local lipid environment around the sterol molecule, thus, reflects how it interacts with the surrounding lipids. To analyze the packing around cholesterol of the fatty acyl chains in our study, a two-dimensional radial distribution function (RDF)

$$g(r_i) = \frac{N(r_i)}{2\pi r_i \rho(r_\infty)} \qquad (2)$$

was generated [57]. In this equation r_i is the distance from a selected atom on the steroid moiety (defined as the central atom) to the carbon atom on an acyl chain (*sn*-1 or -2) of the phospholipid, and $N(r_i)$ is the number of acyl chain carbons inside a bin at distance r_i and at the same depth (±1 Å in the z direction) within the bilayer as the central atom. The term

$$\rho(r_\infty) = \frac{N(r_\infty)}{2\pi r_\infty} \qquad (3)$$

represents the overall density of acyl chain atoms in the membrane, with r_∞ set to 25 Å in practice. C10 and C13 were chosen as the central atom. Of the series of peaks in the RDF obtained (Figure 6), we focus on the first one that reflects the arrangement of the chains closest to a cholesterol molecule.

Differences in the packing around cholesterol for the SA chain at the *sn*-1 position and for the OA and n-3 PUFA chains at the *sn*-2 position are immediately apparent in the RDF calculated with C10 for the central atom (Fig. 6, left panel). The RDF for the SA *sn*-1 chain has a

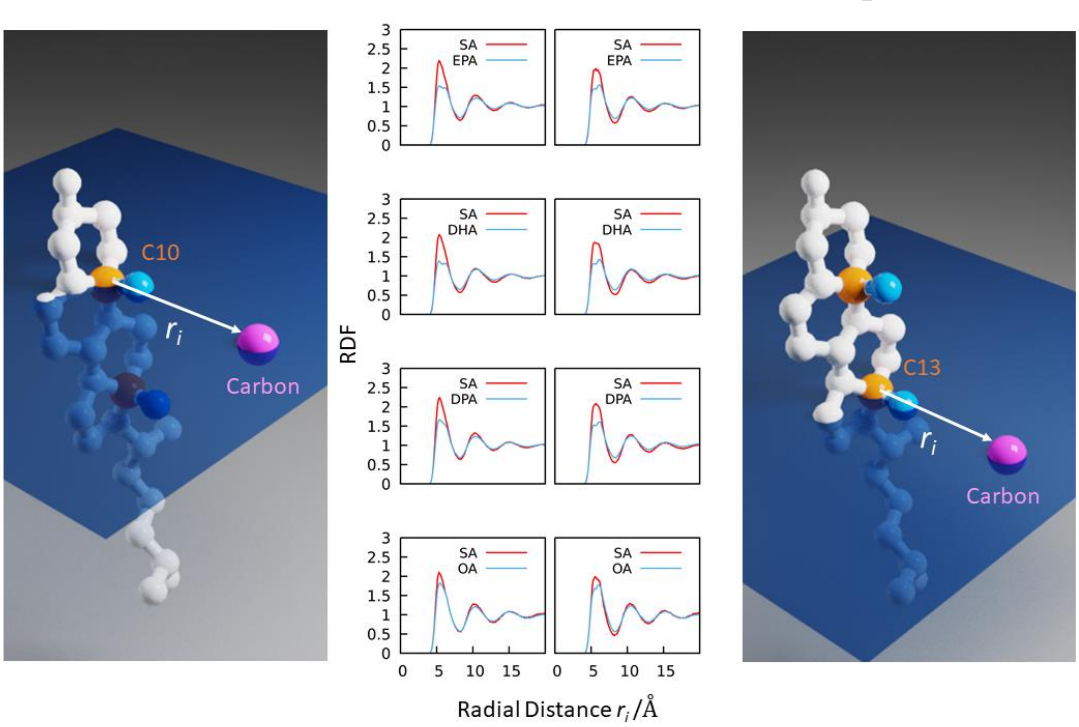

Figure 6 Radial distribution function (RDF) for carbon atoms on the sn-1 and-2 chains of OA-PC, DPA-PC, DHA-PC and EPA-PC around the C10 (left panel) and C13 (right panel) atom on cholesterol. The carbon atoms on cholesterol and phospholipid are at the same depth (within ±1 Å in z direction) as shown in the illustration on two sides. RDF plots relative to the C25 atom on cholesterol can be found in Figure S7 (Supporting Information).

similar shape in each case. The first maximum at a distance of about 6 Å is a well-defined single peak. By contrast, the RDF for the unsaturated *sn*-2 chain differs in each case. In OA-PC the first maximum for the OA chain is reduced in height compared to the SA chain and, suggesting the presence of two peaks that do not precisely overlap, there is a hint of asymmetry. The reduction in height of the first maximum for the DPA chain in DPA-PC is more marked, as is its asymmetry.

There is further reduction in height and a better-defined separation into two peaks for the DHA chain in DHA-PC and the EPA chain in EPA-PC. These observations indicate that the PUFA, and to less extent OA, chains do not pack around cholesterol as tightly as the SA chain. The greater order of the saturated SA chain means that it adopts a more linear conformation that is able to lie parallel to the planar faces of the tetracyclic ring of the sterol. The higher disorder of the OA and, much more markedly, DPA, DHA and EPA chains produces an irregular configuration that is less compatible with close proximity, resulting in a distribution that is more spread out and uneven.

We also calculated RDF lower down the steroid moiety by choosing C13 to be the central atom (Fig. 6, right panel). The first maximum for the *sn*-1 chain in all cases is less sharp than when C10 is the central atom. This change is due to the higher disorder that exists deeper in the bilayer where the C13 position is located. The same argument applies to the shape of the first maximum in the RDF for the *sn*-2 chains. The OA and DPA chains have a first maximum that is more clearly split into two peaks in the case of C13 position because the chains are more disordered. For DHA and EPA the difference between the C10 and C13 cases is less, which we attribute to near uniform high disorder that these chains possess throughout their entire length. A similar overall pattern is retained by RDF calculated about the C25 position in the tail of the sidechain of the sterol (Fig. S7, Supporting Information). Like at the C10 and C13 positions, the differential in height of the first maximum again signifies that all three n-3 PUFA and, to much less extent, OA at the *sn*-2 position do not pack as compactly as saturated SA at the *sn*-1 position. Peaks are not resolved within the maximum because there is greater symmetry in the distribution of phospholipid chains around the cholesterol sidechain.

The sterol ring on cholesterol is not symmetric. It has a planar structure that is flat on one side (α face) and has two methyl groups poking out on the other bumpy side (β face) (Fig. 7, upper panel). Given this molecular structure, the surrounding phospholipid chains are not

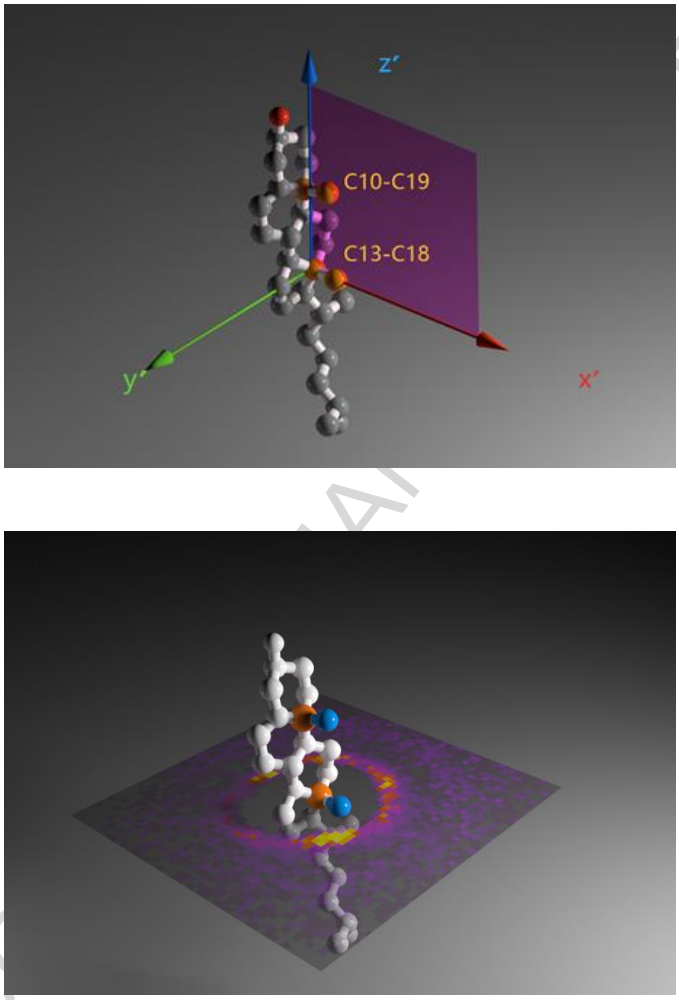

Figure 7 Coordinate system (*x′*,*y′*,*z′*) used in the number density profile (NDP) generation relative to the cholesterol molecule (upper panel) and an example of one slice illustrating the set-up of the NDP relative to cholesterol in OA-PC (lower panel). The color scale is the same as in Fig. 8.

expected to pack equally with respect to the two faces. To map the azimuthal distribution, and so elaborate upon the RDF described above (Fig. 6), we generated a number density profile (NDP)

for the carbon atoms on the acyl chains with respect to an axis system (x',y',z') fixed in the cholesterol molecule. All 20 cholesterol molecules in our simulation were registered to a common frame of reference in which the C13 atom was chosen to be the origin, the C13-C18 vector was fixed on the x' direction and C13-C10 vector was kept in the $x'z'$ plane (Fig. 7, upper panel). The space around sterol molecules was then divided into bins $0.5 \times 0.5 \times 0.5$ Å^3 in size, and the number density of specified atoms on phospholipid molecules in each bin was counted through 180 ns of trajectory using a sampling rate of 50 frames per ns. Because of the consistent registration of coordinates, the NDP for all 20 cholesterol molecules could be simply added up. We computed in this way the NDP for the carbon atoms on the *sn*-1 or -2 chain of phospholipids within 1 nm distance from the origin on cholesterol in each system. A slice taken at $z' = 0$ (Fig. 7, lower panel) illustrates the set-up of the map of the spatial position of N(x',y') obtained.

Two ring-like structures around the cholesterol molecule can be discerned in the NDP for the *sn*-1 (Fig. 8, left column) and -2 chains (Fig. 8, right column) on OA-PC, DPA-PC, DHA-PC and EPA-PC in the slice taken at $z' = 0$. The first (inner) ring, which is 10-12 Å in diameter, maps the distribution of the chains closest to the sterol and follows the shape of the flat α face on the left and the bumpy β face on the right. The second ring, which is approximately 20 Å in diameter, maps the distribution of the chains in the next layer out and is fuzzier. The pattern for the NDP is unique in each case. For OA-PC, the inner ring for the SA and OA chains is thinner and better defined compared to the corresponding chains in the polyunsaturated systems. In addition, the gap between the first and second rings is clearer for the saturated *sn*-1 chain than for the monounsaturated and, more markedly, polyunsaturated *sn*-2 chains. These general features

quantitatively agree with our assessment from the two-dimensional RDF plots - the packing of SA at the *sn*-1 position is tighter around cholesterol than OA and, even more so, DPA, DHA and EPA at the *sn*-2 position.

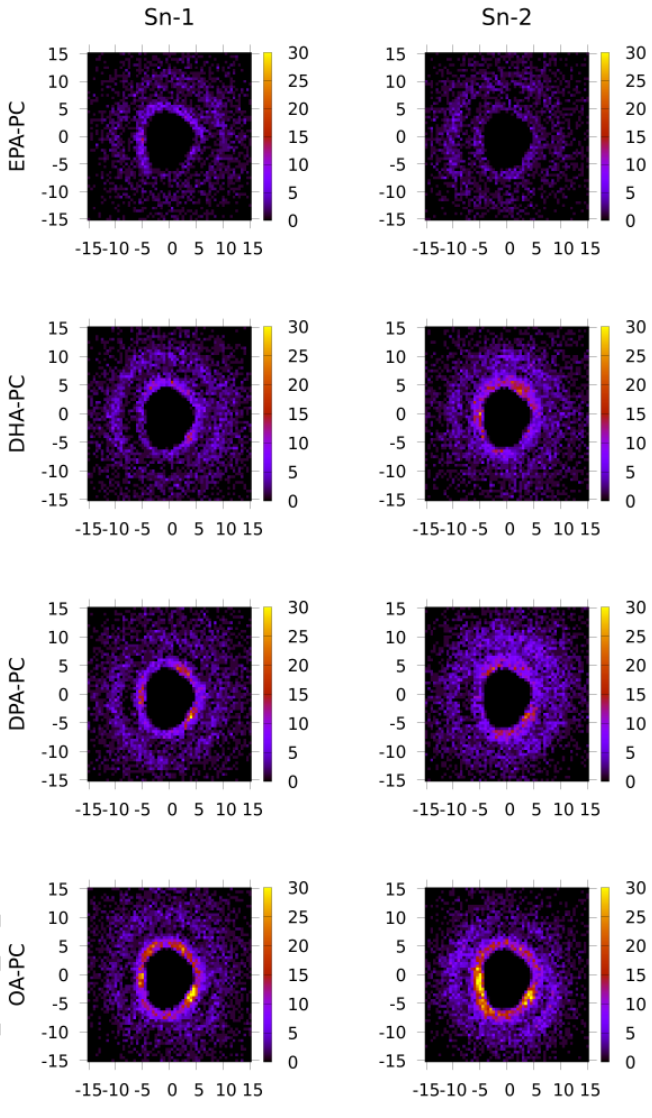

Figure 8 NDP around cholesterol of the carbon atoms on the *sn*-1 (left column) and -2 (right column) chains in OA-PC, DPA-PC, DHA-PC and EPA-PC. Slice is at the depth of the C13 atom on cholesterol. The color represents number of carbons found in $0.5 \times 0.5 \times 0.5$ Å^3 bins in 180 ns by a sampling rate of 50 frames/ns.

The NDP plots also probe how the density of the nearest neighbor chains in the first ring

varies with orientation around the sterol (Fig. 8). Regions of highest density, which indicate where a chain is most likely to be found, are apparent at the 1, 4, 9 and 11 o'clock positions for the SA chain and at the 4 and 7-10 o'clock positions for the OA chain in OA-PC. The region of high density for the latter chain at the 7-10 o'clock positions indicates that to some extent OA favors the flat surface of cholesterol. There is less heterogeneity in density for the more disordered chains in the n-3 PUFA containing membranes. In DPA-PC, the SA and DPA chains have highest density at the 1, 4 and 9 positions and the 4 and 11 positions, respectively. The regions of high density are less pronounced than in OA-PC and, in contrast to the OA chain, the DPA chain does not exhibit any preference for the flat face of the sterol. An almost homogenous distribution of density exists for the SA chain in DHA-PC, while regions of high density occur at the 1 and 9 o'clock positions for the DHA chain. As in DPA-PC, the regions of high density are not as distinct as in OA-PC. In EPA-PC, the most disordered of the three n-3 PUFA-containing membranes, the distribution of both SA and EPA chains ultimately becomes homogenous.

The preference of the OA chain in OA-PC for the flat face of cholesterol exhibited in our NDP plots is contrary to the assessment made in simulations comparing RDF between the CH=CH on the *sn*-2 chain of the phospholipid and CH_3 group at the C13 position on cholesterol in 1-palmitoyl-2-oleoylphosphatidycholine (POPC), which has saturated palmitic acid at the *sn*-1 position and OA at the *sn*-2 position, and 1,2-dioleoylphosphatidylcholine (DOPC), which has OA at *sn*-1 and -2 position, bilayers [58]. In this earlier work greater disparity in height between the first and second peaks in the RDF plot for POPC compared to DOPC was attributed to OA preferring the bumpy face. It is an interpretation, however, made without the definitive insight

into orientation provided by our NDP plots. The higher density for DHA than SA seen in the inner ring closest to cholesterol of our NDP plots with DHA-PC is another observation that contradicts previously published simulations [23]. Probability density distributions around the sterol were calculated showing a shell-like structure, similar to the rings in the NDP plots reported here, in which solvation by SA over DHA is preferred. Possible reasons for the discrepancy between findings include the use in the current simulations of an updated version of the force field (CHARMM36p vs. CHARMM27) and of the more physically realistic NPT ensemble (as opposed to the constant-energy, constant-volume ensemble (NVE)).

3.3 Biological implications

In conclusion, our MD simulations on DPA-PC, DHA-PC and EPA-PC demonstrate that all three n-3 PUFA increase disorder within a membrane and interact less favorably with cholesterol compared to monounsaturated OA in an OA-PC control. Differences between their molecular organization and interaction with cholesterol were revealed. EPA and DPA create most disorder and least disorder, respectively, while the effect of DHA is the same as DPA. The differential in order between them is modest (~5%), as quantified by the average order parameter of the SA chain at the sn-1 position, yet affects their ability to pack close to cholesterol. It is, moreover, of potential significance in understanding the dietary impact of the n-3 PUFA found in fish oils.

The lipid raft concept offers an example of potential sensitivity to the amount of disorder produced by a particular n-3 PUFA. According to this concept, nano-sized domains enriched in

sphingolipid and cholesterol that are liquid ordered (l_o) and contain signaling proteins are surrounded by lipid that is liquid disordered (l_d) in the plasma membrane [12]. When the rafts coalesce together, they become functionalized. A variation on this scenario has incorporation of n-3 PUFA into the phospholipids of the bulk lipid fine tuning the clustering of rafts via the increased differential in order between within raft and non-raft environments that results [18,59]. In support of this proposal, we recorded solid state ^{2}H NMR spectra for deuterated analogs of EPA-, DHA- and OA-containing PC in mixtures with SM and cholesterol (1:1:1 mol) that were analyzed in terms of segregation into SM-rich/cholesterol-rich (raft-like) and PC-rich/cholesterol-poor (non-raft) domains [17]. Two-component spectra indicating slow exchange between domains larger in size ($r > 35$ nm) were obtained with EPA, whereas single component spectra indicating fast exchange between domains smaller in size ($r < 45$ nm) were obtained with OA. Consistent with a smaller reduction in order, spectra indicative of intermediate exchange between domains that fall in size between the limits estimated for EPA and OA were obtained with DHA. Whether signaling proteins in rafts are turned on or off, thus, may depend upon the n-3 PUFA incorporated into membrane phospholipids.

The smaller reduction in order produced by DPA compared to EPA is also a factor that should be borne in mind when assessing the efficacy of EPA. Specifically, fatty acid analyses of the composition of cells treated with EPA have shown that substantial elongation to DPA can occur [7]. In such cases, the increase in disorder anticipated in response to uptake of EPA would be reduced. The similar effect on membrane order, for instance, that was seen in B lymphoma cells treated with EPA and DHA was ascribed in part to elongation of EPA to DPA [37].

Additional biological implications for our work include informing the design of future clinical studies based on sound mechanistic research. EPA, DPA, and DHA are not, for example, bioequivalent for raft-dependent neuronal function in pre-clinical and clinical models [3]. Perhaps differences in molecular structure and interactions with plasma membrane cholesterol can partially explain the distinction in clinical efficacy. There are biological implications, furthermore, outside of lipid rafts. As an example, cardiolipin is a unique phospholipid to which n-3 PUFA are found to be esterified in the inner mitochondrial membrane [60]. Differences in molecular structure between DPA, DHA, and EPA could potentially influence binding kinetics to key respiratory enzymes in the mitochondrial inner membrane and thereby modulate mitochondrial bioenergetics. Plasmalogens, with an ether linkage at the *sn*-1 position and an ester linkage at the *sn*-2 position, are another class of phospholipid enriched in n-3 PUFA implicated in human disease [61]. Their packing, which is tighter than the di-acyl counterpart [62], is likely sensitive to the specific structure of a particular n-3 PUFA. Future studies will need to build on our predictions from simulations to address how EPA/DPA/DHA influences various models of membrane structure-function.

AUTHOR CONTRIBUTIONS

X.L. designed the research, ran and analyzed simulations and wrote the article, J.J.K. performed NMR experiments and analyzed NMR data, A.T.C performed NMR experiments and analyzed NMR data, S.W.C. ran and analyzed simulation and prepared figures, S.R.S designed the research and wrote the article, S.E.F. designed the research and wrote the article, and S.R.W.

designed the research, wrote the article and takes primary responsibility for the final content.

ACKNOWLEDGEMENTS

The work was funded, in part, by a grant from the National Institutes of Health (R01AT008375 to S.R.S.).

REFERENCES

[1] D. Mozaffarian, J.H.Y. Wu, Omega-3 fatty acids and cardiovascular disease: effects on risk factors, molecular pathways and clinical events, J. Am. Coll. Cardiol. 58 (2011) 2047-2067.

[2] H.O. Bang, J. Dyerberg, A. Nielson, Plasma lipid and lipoprotein pattern in Greenlandic West-coast Eskimos, Lancet 297 (1971) 1143–1146.

[3] S.C. Dyall, Long-chain omega-3 fatty acids and the brain: a review of the independent and shared effects of EPA, DPA and DHA, Front. Aging Neurosci. 7 (2015) 52.

[4] P.C. Calder, Omega-3 polyunsaturated fatty acids and inflammatory processes: nutrition or pharmacology? Br. J. Clin. Pharmacol. 75 (2013) 645-662.

[5] A. Binia, C. Vargas-Martínez, M. Ancira-Moreno, L.M. Gosoniu, I. Montoliu, E. Gámez-Valdez, D.C. Soria-Contreras, A. Angeles-Quezada, R. Gonzalez-Alberto, S. Fernández, D. Martínez-Conde, B. Hernández-Morán, M. Ramírez-Solano, C Pérez-Ortega, Y. Rodríguez-Carmona, I. Castan, I. Rubio-Aliaga, F. Vadillo-Ortega, R. Márquez-Velasco, R. Bojalil, J.C. López-Alvarenga, P. Valet, M. Kussmann, I. Silva-Zolezzi, M.E. Tejero, Improvement of cardiometabolic markers after fish oil intervention in young Mexican adults and the role of PPARα L162V and PPARγ2 P12A. J. Nutr. 43 (2017) 98-106.

[6] V.C. Vaughan, H.R. Hassing, P.A. Lewandowski, Marine polyunsaturated fatty acids and cancer therapy, Br. J. Cancer 108 (2013) 486–492.

[7] G. Kaur, D. Cameron-Smith, M. Garg, A.J. Sinclair, Docosapentaenoic acid (22:5n-3): a review of its biological effects, Prog. Lipid Res. 50 (2011) 28–34.

[8] D. Mozaffarian, J.H.Y. Wu, (n-3) Fatty acids and cardiovascular health: are effects of

EPA and DHA shared or complementary? J. Nutr. 142 (2012) 614S–625S.

[9] P.C. Calder, Marine omega-3 fatty acids and inflammatory processes: Effects, mechanisms and clinical relevance, Biochim. Biophys. Acta 1851 (2015) 469–484.

[10] T.Y. Hou, D.N. McMurray R.S. Chapkin, Omega-3 fatty acids, lipid rafts, and T cell signaling, Eur. J. Pharmacol. 785 (2016) 2-9.

[11] S.R. Shaikh, Biophysical and biochemical mechanisms by which dietary N-3 polyunsaturated fatty acids from fish oil disrupt membrane lipid rafts, J. Nutr. Biochem. 23 (2012) 101-105.

[12] D. Lingwood, K. Simons, Lipid rafts as a membrane-organizing principle, Science 327 (2010) 46–50.

[13] B.D. Rockett, H. Teague, M. Harris, M. Melton, J. Williams, S.R. Wassall, S.R. Shaikh, Fish oil increases raft size and membrane order of B cells accompanied by differential effects on function, J. Lipid Res. 53 (2012) 674-685.

[14] H.F. Turk, R.S Chapkin, Membrane lipid raft organization is uniquely modified by n-3 polyunsaturated fatty acids, Prost. Leuk. Essent. Fatty Acids 88 (2013) 43–47.

[15] S.R. Shaikh, A.C. Dumaual, A. Castillo, D LoCascio, R.A. Siddiqui, W. Stillwell, S.R. Wassall, Oleic and docosahexaenoic acid differentially phase separate from lipid raft molecules: A comparative NMR, DSC, AFM, and detergent extraction study, Biophys. J. 87 (2004) 1752-1766.

[16] S.P. Soni, D.S. LoCascio, Y. Liu, J.A. Williams, R. Bittman, W. Stillwell, S.R. Wassall, Docosahexaenoic acid enhances segregation of lipids between raft and non-raft domains: ^{2}H

NMR study, Biophys. J. 95 (2008) 203-214.

[17] J.A Williams, S.E. Batten, M. Harris, B.D. Rockett, S.R. Shaikh, W. Stillwell, S.R. Wassall, Docosahexaenoic and eicosapentaenoic acids segregate differently between raft and non-raft domains, Biophys. J. 103 (2012) 228-237.

[18] S.R. Shaikh, J.J. Kinnun, X. Leng, J.A. Williams, S.R Wassall, How polyunsaturated fatty acids modify molecular organization in membranes: insight from NMR studies of model systems, Biochim. Biophys. Acta 1848 (2015) 211-219.

[19] R.W. Pastor, A.D. MacKerell Jr., Development of the CHARMM force field for lipids, J. Phys. Chem. Lett. 2 (2012) 1526-1532.

[20] L. Saiz, M.L. Klein, Structural properties of a highly polyunsaturated lipid bilayer from molecular dynamics simulations, Biophys. J. 81 (2001) 201-216.

[21] S.E. Feller, K. Gawrisch, A.D. MacKerell Jr., Polyunsaturated fatty acids in lipid bilayers: intrinsic and environmental contributions to their unique physical properties, J. Amer. Chem. Soc. 124 (2002) 318-326.

[22] T. Huber, K. Rajamoorthi, V.F. Kurze, K. Beyer, M.F. Brown, Structure of docosahexaenoic acid-containing phospholipid bilayers as studied by ^{2}H NMR and molecular dynamics simulations, J. Amer. Chem. Soc. 124 (2002) 298-309.

[23] M.C. Pitman, F. Suits, A.D. MacKerell Jr., S.E. Feller, Molecular-level organization of saturated and polyunsaturated fatty acids in a phosphatidylcholine bilayer containing cholesterol, Biochemistry 43 (2004) 15318-15328.

[24] S.R. Shaikh, V. Cherezov, M. Caffrey, S.P. Soni, D. LoCascio, W. Stillwell, S.R.

Wassall, Molecular organization of cholesterol in unsaturated phosphatidylethanolamines: X-ray diffraction and solid state ^{2}H NMR reveal differences with phosphatidylcholines, J. Amer. Chem. Soc. 128 (2006) 5375-5383.

[25] W. Stillwell, S.R. Wassall, Docosahexaenoic acid: membrane properties of a unique fatty acid, Chem. Phys. Lipids 126 (2003) 1–27.

[26] S. Jo, J.B. Lim, J.B. Klauda, W. Im, CHARMM-GUI MEMBRANE BUILDER for mixed bilayers and its application to yeast membranes, Biophys. J. 97 (2009) 50-58.

[27] J.B. Klauda, V. Monje, T. Kim, W. Im, Improving the CHARMM force field for polyunsaturated fatty acid chains, J. Phys Chem. B 116 (2012) 9424-9431.

[28] T. Darden, D. York, L. Pedersen, Particle mesh Ewald: an $n \cdot \log(n)$ method for Ewald sums in large systems, J. Chem. Phys. 98 (1993) 10089-10092.

[29] B.R. Brooks, C.L. Brooks III, A.D. MacKerell Jr., L. Nilsson, R.J. Petrella, B. Roux, Y. Won, G. Archontis, C. Bartels, S. Boresch, A. Caflisch, L. Caves, Q. Cui, A.R. Dinner, M. Feig, S. Fischer, J. Gao, M. Hodoscek, W. Im, K. Kuczera, T. Lazaridis, J. Ma, V. Ovchinnikov, E. Paci, R.W. Pastor, C.B. Post, J.Z. Pu, M. Schaefer, B. Tidor, R.M. Venable, H.L. Woodcock, X. Wu, W. Yang, D.M. York, M. Karplus, CHARMM: the biomolecular simulation program, J. Comp. Chem. 30 (2009) 1545-1614.

[30] J.C. Phillips, R. Braun, W. Wang, J. Gumbart, E. Tajkhorshid, E. Villa, C. Chipot, R.D. Skeel, L. Kalé, K. Schulten, Scalable molecular dynamics with NAMD, J. Comp. Chem. 26 (2005) 1781-1802.

[31] S.E. Feller, Y. Zhang, R.W. Pastor, B.R. Brooks, Constant pressure molecular dynamics

simulation: the Langevin piston method, J. Chem. Phys. 103 (1995) 4613-4621.

[32] W. Humphrey, A. Dalke, K. Schulten, VMD - Visual Molecular Dynamics, *J. Mol. Graph.* 14 (1996) 33-38.

[33] L.S. Vermeer, B.L. De Groot, V. Réat, A. Milon, J. Czaplicki, Acyl chain order parameter profiles in phospholipid bilayers: computation from molecular dynamics simulations and comparison with ^{2}H NMR experiments, Eur. Biophys. J. 36 (2007) 919-931.

[34] J. Seelig, Deuterium magnetic resonance theory and application to lipid membranes, Q. Rev. Biophys.10 (1977) 353-418.

[35] A.K. Engel, D. Cowburn, The origin of multiple quadrupole couplings in the deuterium NMR spectra of the 2 chain of 1,2 dipalmitoyl-sn-glycero-3-phosphorylcholine, FEBS Lett. 126 (1981) 169-171.

[36] L.L. Holte, S.A. Peter, T.M. Sinnwell, K. Gawrisch, ^{2}H nuclear magnetic resonance order parameter profiles suggest a change of molecular shape for phosphatidylcholines containing a polyunsaturated acyl chain, Biophys. J. 68 (1995) 2396-2403.

[37] M. Harris, J.J. Kinnun, R. Kosaraju, X. Leng, S.R. Wassall, S.R Shaikh, Membrane disordering by eicosapentaenoic acid in B lymphomas is reduced by elongation to docosapentaenoic acid as revealed with solid-state nuclear magnetic resonance spectroscopy of model membranes, J. Nutr. 146 (2016) 1283-1289.

[38] N.V. Eldho, S.E. Feller, S. Tristram-Nagle, I.V. Polozov, K. Gawrisch, Polyunsaturated docosahexaenoic vs. docosapentaenoic acid-differences in lipid matrix properties from the loss of one double bond, J. Amer. Chem. Soc. 25 (2003) 6409–6421.

[39] K. Rajamoorthi, H.I. Petrache, T.J. McIntosh, M.F. Brown, Packing and viscoelasticity of polyunsaturated ω-3 and ω-6 lipid bilayers as seen by ^{2}H NMR and X-ray diffraction, J. Amer. Chem. Soc. 127 (2005) 1576-1588.

[40] J. Seelig, N. Waespe-Sarcevic, Molecular order in cis and trans unsaturated phospholipid bilayers, Biochemistry 17 (1978) 3310-3315.

[41] S.P. Soni, J.A. Ward, S.E. Sen, S.E. Feller, S.R. Wassall, Effect of *trans* unsaturation on molecular organization in a phospholipid membrane, Biochemistry 48 (2009) 11097-11107.

[42] S.E. Feller, Acyl chain conformations in phospholipid bilayers: a comparative study of docosahexaenoic acid and saturated fatty acids, Chem. Phys. Lipids 153 (2008) 76-80.

[43] O. Soubias, K. Gawrisch, Docosahexaenoyl chains isomerize on the sub-nanosecond timescale, J. Am. Chem. Soc. 129 (2007) 6678-6679.

[44] K. Gawrisch, O. Soubias, Structure and dynamics of polyunsaturated hydrocarbon chains in lipid bilayers—significance for GPCR function, Chem. Phys. Lipids 153 (2008) 64-75.

[45] X. Leng, J.J. Kinnun, D. Marquardt, M. Ghefli, N. Kučerka, J. Katsaras, J. Atkinson, T.A. Harroun, S.E. Feller, S.R. Wassall, α-Tocopherol is well designed to protect polyunsaturated phospholipids: MD simulations, Biophys. J. 109 (2015) 1608-1618.

[46] A.R. Braun, E.G. Brandt, O. Edholm, J.F. Nagle, J.N. Sachs, Determination of electron density profiles and area from simulations of undulating membranes, Biophys. J. 100 (2011) 2112-2120.

[47] N. Kučerka, F.A. Heberle, J. Pan, J. Katsaras, Structural significance of lipid diversity as studied by small angle neutron and X-ray scattering, Membranes 5, (2015) 454-472.

[48] P. Heftberger, B. Kollmitzer, F.A. Heberle, J. Pan, M. Rappolt, H. Amenitsch, N. Kučerka, J. Katsaras, G. Pabst, Global small-angle X-ray scattering data analysis for multilamellar vesicles: the evolution of the scattering density profile model, J. Appl. Cryst. 47 (2014) 173-180.

[49] D. Marquardt, F.A. Heberle, D.V. Greathouse, R.E. Koeppe II, R.F. Standaert, B.J. Van Oosten, T.A. Harroun, J.J. Kinnun, J.A. Williams, S.R. Wassall, J. Katsaras, Lipid bilayer thickness determines cholesterol's location in model membranes, Soft Matter 12 (2016) 9417-9428.

[50] H.I. Petrache, S.W. Dodd, M.F. Brown, Area per lipid and acyl chain length distributions in fluid phosphatidylcholines determined by ^{2}H NMR spectroscopy, Biophys. J. 78 (2000) 3172–3192.

[51] D. Marquardt, N. Kučerka, S.R. Wassall, T.A Harroun, J. Katsaras, J. Cholesterol's location in lipid bilayers, Chem. Phys. Lipids 99 (2016) 17-25.

[52] D. Huster, K. Arnold, K. Gawrisch, Influence of docosahexaenoic acid and cholesterol on lateral lipid organization in phospholipid mixtures, Biochemistry 37 (1998) 17299-17308.

[53] M. Mihailescu, O. Soubias, D. Worcester, S.H. White, K. Gawrisch, Structure and dynamics of cholesterol-containing polyunsaturated lipid membranes studied by neutron diffraction and NMR, J. Membrane Biol. 239 (2011) 63-71.

[54] W-C. Hung, M-T. Lee, F-Y. Chen, H.W. Huang, The condensing effect of cholesterol in lipid bilayers, Biophys. J. 92 (2007) 3960–3967.

[55] E. Oldfield, M. Meadows, D. Rice, R. Jacobs, Spectroscopic studies of specifically

deuterium labeled membrane systems. Nuclear magnetic resonance investigation of the effects of cholesterol in model systems, Biochemistry 17 (1978) 2727-2740.

[56] M.R. Brzustowicz, W. Stillwell, S.R. Wassall, Molecular organization of cholesterol in polyunsaturated phospholipid membranes: a solid state ^{2}H NMR investigation, FEBS Lett. 451 (1999) 197-202.

[57] T. Róg, M. Pasenkiewicz-Gierula, I. Vattulainen, M. Karttunen, What happens if cholesterol is made smoother: importance of methyl substituents in cholesterol ring structure on phosphatidylcholine–sterol interaction, Biophys. J. 92 (2007) 3346-3357.

[58] S.A. Pandit, S.W. Chiu, E. Jakobsson, A. Grama, H.L. Scott, Cholesterol packing around lipids with saturated and unsaturated chains: a simulation study, Langmuir 24 (2008) 6858-6865.

[59] K. R. Levental, J.H. Lorent, X. Lin, A.D. Skinkle, M.A. Surma, E.A. Stockenbojer, A.A. Gorfe, I. Levental, Polyunsaturated lipids regulate membrane domain stability by tuning membrane order, Biophys. J. 110 (2016) 1800–1810.

[60] S.R Shaikh, D.A. Brown, Models of plasma membrane organization can be applied to mitochondrial membranes to target human health and disease with polyunsaturated fatty acids, Prost. Leuk. Essent. Fatty Acids 88 (2013) 21-28.

[61] N.E. Braverman, A.B. Moser, Functions of plasmalogen lipids in health and disease, Biochim. Biophys. Acta 1822 (2012) 1442-1452.

[62] T. Rog, A. Koivuniemi, The biophysical properties of ethanolamine plasmalogens revealed by atomistic molecular dynamics simulations, Biochim. Biophys. Acta 1858 (2016) 97-103.

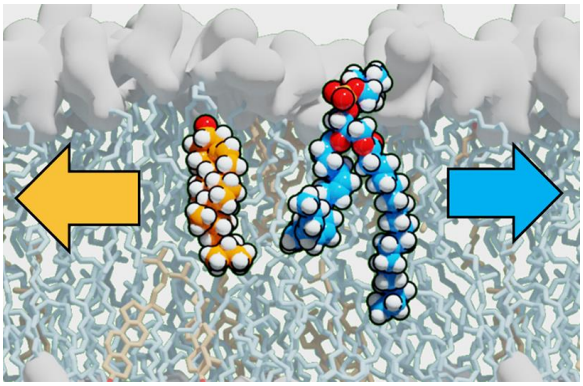

Highly disordered

n-3 PUFA deter close

packing to cholesterol

EPA>DHA≥DPA

Graphical abstract

Highlights

- **n-3 PUFA disorder membranes**
- **Disordering depends upon number of double bonds and chain length, EPA (20:5) > DHA (22:6) ≥ DPA (22:5)**
- **Higher disorder prevents closer packing with cholesterol**
- **EPA, DHA and DPA are not equivalent in their interactions with membranes**